ELSEVIER

Journal of Nuclear Materials 258–263 (1998) 1557–1561

journal of nuclear materials

Fiber creep rate and high-temperature properties of SiC/SiC composites

C.A. Lewinsohn *, R.H. Jones, G.E. Youngblood, C.H. Henager Jr.

Pacific Northwest National Laboratory, Richland, Washington 99352, USA

Abstract

Optimization of the high-temperature structural properties of continuous silicon carbide fiber, silicon carbide matrix composites (SiC/SiC) requires a fundamental understanding of the relationship between fiber, matrix, and interface properties. Results of a study aimed at relating the fiber creep rate to the subcritical crack growth (SCG) rate and fracture properties of SiC/SiC composites have demonstrated that the crack growth rate in a bulk composite is controlled by the fiber creep rate. This result was demonstrated for Nicalon–CG and Hi–Nicalon fiber reinforced material where a 100°C shift in the creep strength of the fiber resulted in a similar shift in the crack growth rate of the composite. Irradiation enhanced creep of SiC fibers and matrix must also be considered in the performance assessment of SiC/SiC composites. An estimate of the impact of irradiation creep of SiC fibers on the SCG of SiC/SiC will be presented.

1. Introduction

Bridged cracks may exist in SiC/SiC components used below the known matrix fracture stress after accidental overloads, impact damage during service, or as flaws resulting from processing. In addition, bridged cracks may occur at service stresses around notches and holes, or matrix cracks may occur due to creep. Thus, bridged cracks may exist in SiC/SiC even under service conditions that are constrained by accumulation of creep damage or dimensional change due to creep. Fracture of components containing bridged cracks is governed by the time-dependent bridging stresses exerted by the fibers crossing the crack that are able to sustain loads [1–3]. Creep of fibers that bridge cracks in ceramic matrix-composites (CMC) causes subcritical crack growth (SCG) [1–4]. To determine the lifetime and environmental sensitivity of these materials it is essential to understand this type SCG.

Numerous microstructural and environmental parameters can influence subcritical crack growth in SiC/SiC composites. Due to the complex nature of the SiC/SiC materials it is not possible to predict the influence of each of these variables without experimental verification. This paper will describe an experimental investigation of the effects of fiber creep rate and interface thickness on the subcritical crack growth rate of SiC/SiC composites intended for fusion energy system applications. The goal of the investigation is to identify critical parameters that can be manipulated during composite fabrication to provide the optimum lifetime of components in service conditions.

Very little data has been published regarding the creep of silicon carbide during irradiation [5–7]. This limited data suggests that irradiation enhances creep in silicon carbide and, hence, the effect of irradiation-enhanced fiber creep on SCG in SiC/SiC must be considered. Although there is no data currently available that describes the irradiation creep of Nicalon™ fibers, the irradiation creep behavior will be estimated by assuming that irradiation will cause a similar order of magnitude increase in the fiber creep rate as in monolithic (unreinforced) silicon carbide. The estimated increase in fiber creep rate will be used to estimate an increase in composite subcritical crack growth rate.

* Corresponding author. Tel.: +1-509-372-0268; fax: +1-509-376-0418; e-mail: ca_lewinsohn@pnl.gov.

0022-3115/98/$19.00
PII: S0022-3115(98)00218-9

2. Experimental method

The experimental approach has been described in detail elsewhere [2], but will be summarized. The tests described were conducted in gettered argon. The argon was initially 99.999% pure, and the oxygen content was lowered to less than 20 ppm by passing the gas through a titanium gettering furnace. Subcritical crack growth was obtained by loading single-edge-notched beam (SENB) bend-bar specimens in 1/4 four-point bending in a fully articulated, sintered silicon carbide fixture. The deflection of the specimen midpoint was measured via an alumina pushrod attached to a strain-gage extensometer. The displacements were corrected for differences between the load-point and mid-point and for the compliance of the test apparatus using a method described previously [2]. The specimen and fixture were contained in a vertically oriented mullite tube. The atmosphere inside the mullite tube could be controlled. The fixture was loaded by silicon carbide rods that entered the tube through stainless steel bellows. One of the loading rods was attached to a conventional, strain-gauged cantilever-beam load cell, and the other was attached to the crosshead of an electromechanically controlled, rigid mechanical test frame. [1] The temperature, load, and deflection were continuously monitored by a personal computer with a data acquisition board and analog-to-digital conversion software. [2]

SiC/SiC composite containing Hi–Nicalon™ fibers was examined in this study and compared to the results of previous studies [1–4] that investigated similar material containing Ceramic-grade Nicalon™ fibers. Nicalon™ fibers [3] are a class of silicon carbide fibers derived from polymeric precursors. The fibers consist of varying amounts of amorphous material containing excess carbon and/or oxygen and nanocrystalline grains of silicon carbide [8,9]. The Hi–Nicalon™ fibers are cured by an electron-beam process that inhibits the amount of residual oxygen in the as-produced fibers. It is well known that excess oxygen promotes the thermal decomposition of the fibers and reduces their high-temperature strength [9]. The composite materials were fabricated from 2-dimensional, plain-weave fiber mats. [4] Before matrix infiltration, a 1 μm thick carbon layer was deposited on the fibers via chemical vapor deposition (CVD). The matrix was also deposited by CVD in a process known as chemical vapor infiltration (CVI). The outer surfaces of each bend-bar were coated with a 2 μm thick layer of silicon carbide, deposited by CVD, to provide oxidation resistance and to protect the surfaces from damage.

The materials containing Hi–Nicalon™ fibers will be abbreviated as "Hi–C" to indicate the fiber type and the interface composition. The material that was studied previously will be abbreviated "CG–C". The CG–C material was coated with silicon carbide before fabricating the bend-bar samples, and therefore the bend-bars only had protective coatings on the tensile and compressive surfaces. A third group of specimens were fabricated with Ceramic-grade fibers and a 0.15 μm thick carbon interface, but were otherwise similar to the Hi–C materials, they will be referred to as "CG–C150". The microstructure of the composites reinforced with the Hi–Nicalon™ fibers is shown in Fig. 1. The resulting composites contained approximately 40 volume fraction fibers and 10–15% porosity. Some typical properties of

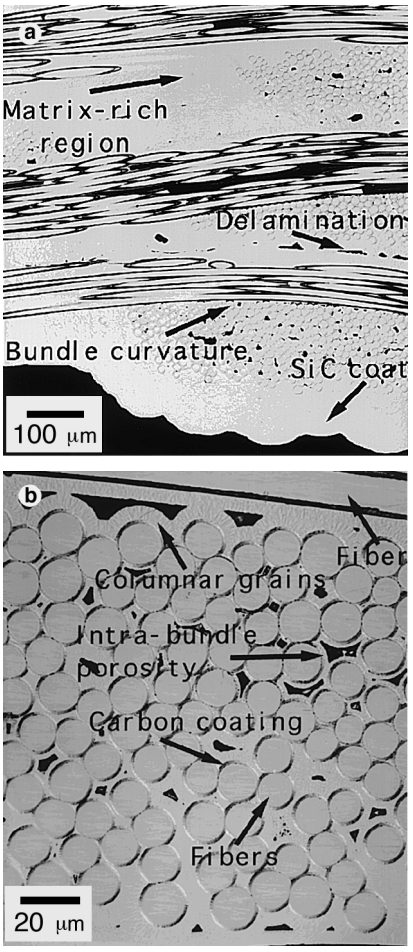

Fig. 1. Typical views of the microstructure of the silicon carbide composites, specifically Hi–C, investigated in this study.

[1] Instron 4400, Instron Corporation, Canton, MA, USA.

[2] LabView, National Instruments Corporation, Austin, TX, USA.

[3] Manufactured by Nippon Carbon, Tokyo, Japan.

[4] Hi–C and CG–C150 Composite fabrication performed by E.I. DuPont Nemours, Wilmington, DE, USA. CG–C composite fabrication performed by RCI (now Hypertherm), Whittier, CA.

Table 1
Physical properties of the materials tested

	CG–C	CG–C150	Hi–C
Fiber type	Ceramic-grade Nicalon	Ceramic-grade Nicalon	Hi–Nicalon
Fiber coating	1.01 ± 0.05 μm Carbon	0.15 μm Carbon	1.0 ± 0.5 μm Carbon
Fibers/tow	420	420	321
Fiber diameter	14.0 ± 0.5 μm	14.0 ± 0.5 μm	14 ± 2.3 μm
Fiber vol. fraction	40	40	40
Composite coating	CVD silicon carbide	CVD silicon carbide	CVD silicon carbide
Porosity	20 ± 5%	Unknown	6 ± 1.4%
Modulus [a]	98 ± 6.6 G Pa	164 ± 10 G Pa	183 ± 18 G Pa
Fracture toughness	17.5 MPa $m^{1/2}$	17.0 ± 0.5 MPa $m^{1/2}$	22.4 ± 0.1 MPa $m^{1/2}$

[a] The modulus is calculated from the specimen compliance measured from the linear portion of loading during flexural testing of SENB specimens at elevated temperature and corrected for fixture compliance.
Variability given as 95% confidence intervals.

the materials discussed in this paper are given in Table 1.

The SENB specimens contained an initial notch, a_0, with a crack length-to-width ratio (a/W) of approximately 0.2. The notch was made using a high-speed diamond saw and was typically 390 mm wide at the tip of the notch and 590 mm wide at the mouth. No attempt was made to sharpen the notch. Specimens were heated at a rate of about 15°C/min up to the test temperature and were allowed to equilibrate for 20 min. Then a load that was calculated [10] to provide an initial applied stress intensity of 10 MPa-$m^{1/2}$ was applied to the sample and held for the duration of the test. This load varied from 540 to 570 N, corresponding to a stress of approximately 150 MPa on the tensile surface of an unnotched beam of the same dimension. Specimens reinforced with Hi–Nicalon™ fibers were tested at 1100°C, 1150°C, 1175°C, and 1200°C and compared to specimens tested at 1100°C that were reinforced with Ceramic-grade Nicalon™ fibers.

3. Results

The displacement of the specimens was corrected for the compliance of the test apparatus, and the compliance of the test specimen was calculated. This compliance was converted to a crack length using the procedure described previously [2] based on experimentally measured crack length versus compliance data. The effective stress intensity factor at the crack tip was determined from the standard formula for a single-edge-notched-beam in four-point loading [10] and the calculated crack length. Previous results [2] have shown that although this procedure under-predicts actual crack lengths, the effects of multiple cracks emanating from the notch tip increases the specimen compliance such that the effective crack velocities reflect the true crack velocities in the damage zone.

The crack velocity as a function of effective stress intensity is shown in Fig. 2 for the Hi–C and CG–C materials. In addition, data for a sintered alpha-silicon

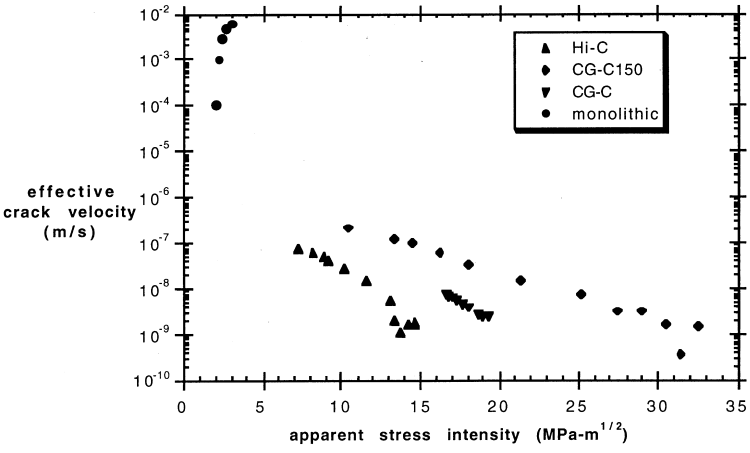

Fig. 2. Comparison of the dependency of crack velocity on apparent stress intensity, at 1373 K in gettered argon, among Hi–C, CG–C150, CG–C, and monolithic silicon carbide.

carbide material that was tested at 900°C are also shown [11]. The sintered alpha-silicon carbide exhibited both stage-II and stage-III behavior under the conditions studied. The sintered alpha-silicon carbide material exhibited slow-crack-growth due to viscous sliding of the grain boundaries, and crack growth in this material is much faster than the silicon carbide composites studied, even at a lower temperature.

4. Discussion

The shapes of the displacement versus time curves for the Hi–C composite were similar to those of the previously tested CG–C materials that exhibited slow-crack-growth controlled by time-dependent relaxation of the fiber-bridging stresses due to fiber creep [1–3]. The temperature dependency of the slow crack growth rate for the CG–C material was approximately 500 kJ/mol which is in close agreement with the reported value for the creep rate of Ceramic-grade fibers. An activation energy of 410 kJ/mol for subcritical crack growth in the Hi–C composites was calculated using the method due to Sherby and Dorn [12–14] using data from compact tension specimens [15]. The subcritical crack growth behavior of the compact tension specimens was identical to that of the single edge-notched beam specimens used in this study [15]. The temperature dependency of the crack velocity for the Hi–C specimens, 410 kJ/mol, was in the range of values reported by Bodet et al. [16] in a thorough study of the creep behavior of Nicalon™ fibers. The crack velocity in the CG–C composites at 1100°C in argon was very close to that of the Hi–C materials at 1150–1175°C (Fig. 2), this roughly corresponds to the temperature differential shown by DiCarlo et al. [17] to obtain the same relaxation in 1 h bend stress relaxation (BSR) tests in the two fibers. The published creep equations for Ceramic-grade Nicalon [18] and Hi-Nicalon [16] predict about 100 K temperature differential to reach 1% creep strain in 300 h for an applied stress of 500 MPa.

Previous investigations of slow crack growth in Ceramic-grade Nicalon™ fiber-reinforced silicon carbide composites, by Henager and Jones [1–3], showed that fiber creep, leading to relaxation of the crack-bridging stresses, accounted for the crack growth rate at 1100°C in argon. The crack-tip stress intensity and crack-opening displacement were time-dependent. Further studies by the same authors [2] have confirmed that fiber creep is responsible for the observed slow crack growth and have shown that a 2-dimensional micromechanics model is capable of predicting the measured effective crack velocities, the time dependence of the crack velocity, and the transition for stage-II type slow crack growth (crack velocity is independent of applied stress intensity) to stage-III crack growth (power-law dependency of crack velocity to applied stress intensity). Therefore, it appears that the subcritical crack growth rate, $\dot{a}$ (m/s), of the Hi–C materials is also controlled by fiber creep rate, $\dot{\varepsilon}_f$ (s^{-1}), and that the fiber creep rate controls the temperature dependency of the crack growth rate,

$$\frac{\dot{a}(T_2)}{\dot{a}(T_1)} = \frac{\dot{\varepsilon}_f(T_2)}{\dot{\varepsilon}_f(T_1)} = \left\{ \exp\left(\frac{Q_f}{R}\left[\frac{1}{T_1} - \frac{1}{T_2} \right] \right) \right\}, \quad (1)$$

where T represents absolute temperature (K), Q_f, represents the activation energy for fiber creep (kJ/mol), and R represents the universal gas constant (8.3144 J-mol/K)

The effective crack velocity of CG–C150 was also measured at 1373 K in argon (Fig. 2). The fiber volume fraction and composition of this material was nominally the same as that of the other materials in this study. The crack velocity of this material was faster than the CG-C materials with a 1 μm-thick interphase. According to linear shear-lag models [19–21], as the thickness of the fiber matrix interphase decreases, the shear stress across the interphase increases. The stresses on bridging fibers with thinner interphases would be higher than those with thicker interphases causing the fibers to creep more, in a given length of time, because of the linear stress dependence for fiber creep. Greater fiber creep would lead to greater decreases in the bridging stresses, and a higher subcritical crack growth rate, as seen by comparison of the CG–C material, that contains fibers with higher creep rates than Hi–Nicalon™ fibers, and the Hi–C material.

In addition to increased fiber bridging-stresses due to thin interphases, a stronger fiber/matrix interfacial bond would also lead to higher fiber stresses than a weaker one. Fast fracture experiments discussed elsewhere [22] and a study conducted by Chawla et al. [23] of the surface roughness, measured by atomic force microscopy, of Ceramic-grade and Hi–Nicalon fibers indicate that the fiber clamping stresses in the Hi–C material are larger than in the CG–C material. Therefore, although the lower creep rate of the Hi–Nicalon fibers relative to the Nicalon–CG fibers should lower the effective crack velocity, the higher interfacial debond energy of the Hi–C material would increase the effective crack velocity. This may explain the difference, discussed earlier, between the reported temperature differential for equivalent creep rates in the Ceramic-grade and Hi–Nicalon fibers, 100 K [17] as discussed earlier, and the lower temperature differential between the measured subcritical crack growth rate in the CG–C and Hi–C materials, 50–75 K. Although some of this difference may be caused by fiber variability and stochastic features of the different experiments, a strong fiber/matrix interfacial bond in the Hi–C material would increase the subcritical crack growth rate and lead to an apparent decrease in the temperature differential for equivalent crack growth rates. Thus, although high fiber bridging stresses

decrease the magnitude of the stress intensity at the crack tip they increase the rate at which the crack tip stress intensity increases due to fiber creep. Further experiments and modeling are required to understand these complex relationships.

As mentioned earlier, there is very little reliable data illustrating the effect of irradiation on the creep behavior of silicon carbide [5–7]. In one of these previous studies [5], oriented graphite substrates were coated with pyrolytic β-silicon carbide and then irradiated at 640°C and 900°C at exposures of 3.2×10^{21} and 3.8×10^{21} nvt ($E > 0.18$ MeV), respectively. Irradiation-induced swelling of the substrate put the silicon carbide in tension causing residual curvature from which the contribution due to irradiation creep could be deduced. These experiments provided rough estimates of the upper bounds of the steady state creep rate.

The steady state creep, ΔE_c, was assumed to be linearly proportional to the product of stress, σ, and fluence, φ,

$$\Delta E_c = K\sigma\varphi. \tag{2}$$

For a hypothetical stress of 100 MPa and a fluence of 10 dpa at the end of about one year, the maximum steady state creep rate, $d\varepsilon_c/dt$, would be 2×10^{-11} s^{-1} at 900°C ($E > 0.18$ MeV). The equivalent steady state creep rate of CVD silicon carbide due to thermal effects at the same stress and temperature would be 1.05×10^{-13} s^{-1} according to data published by Carter et al. [24]. Therefore, irradiation may enhance the thermal creep of CVD silicon carbide by about two orders of magnitude. If irradiation enhanced the creep rate of Nicalon™ fibers by a similar order of magnitude a similar increase in the subcritical crack growth rate in SiC/SiC composites would occur, according to Eq. (1). Additional data on the irradiation-enhanced creep rate of silicon carbide, SiC/SiC composites, or Nicalon™ fibers would allow confirmation of this initial estimate. Clearly, the creep rate of fibers used in SiC/SiC composites intended for structural applications in radiation environments should be minimized to mitigate premature failure due to subcritical crack growth.

5. Conclusions

Subcritical crack growth in SiC/SiC composites is controlled by fiber creep. Lower subcritical crack growth rates require fibers with lower creep rates and an optimum fiber/matrix interfacial bond strength. Additional data concerning the irradiation-enhanced creep of silicon carbide, SiC/SiC or Nicalon™ fibers would aid in evaluating the susceptibility of SiC/SiC to undergo subcritical crack growth in fusion energy system applications. Initial estimation, based on a single data set, of the effect of irradiation on subcritical crack growth in SiC/SiC materials suggests that the crack growth rates will be several orders of magnitude higher than those due to thermal fiber creep alone.

Acknowledgements

This work was also supported by the US Department of Energy (DOE) contract DE-AC06-76RLO 1830 with Pacific Northwest National Laboratory, which is operated for DOE by Battelle.

References

[1] C.H. Henager Jr., R.H. Jones, Ceram. Eng. Sci. Proc. 13 (1992) 411.
[2] C.H. Henager Jr., R.H. Jones, J. Am. Ceram. Soc. 77 (1994) 2381.
[3] C.H. Henager Jr., R.H. Jones, Ceram. Eng. Sci. Proc. 14 (1993) 408.
[4] C.H. Henager Jr., R.H. Jones, Mater. Sci. Eng. A 166 (1993) 211.
[5] R.J. Price, General Atomic Division of General Dynamics Report GA-8200 (1967) 91.
[6] R.J. Price, Nucl. Technol. 35 (1977) 320.
[7] R. Scholz, A. Frias Rebelo, P. Dos Santos, Proceedings of the IEA Workshop on Fusion Materials, Ispra, Italy, 1996.
[8] G. Simon, A.R. Bunsell, J. Mater. Sci. 19 (1984) 3649.
[9] H. Ichikawa, K. Okamura, T. Seguchi, Ceram. Trans. 58 (1995) 65.
[10] ASTM E 399-90, Am. Soc. Testing and Mater., 1990, ASTM, Philadelphia, PA.
[11] K.D. McHenry, R.E. Tressler, J. Am. Ceram. Soc. 63 (1980) 152.
[12] O.D. Sherby, J.E. Dorn, Trans. AIME 9 (1952) 959.
[13] O.D. Sherby, R.L. Orr, J.E. Dorn, Trans. AIME 11 (1954) 71.
[14] C.A. Lewinsohn, C.E. Bakis, R.E. Tressler, ASTM Spec. Tech. Pub. STP 1290 (1996) 9.
[15] C.A. Lewinsohn, C.H. Henager Jr., R.H. Jones, Cer. Eng. Sci. Proc. 18 (1997) 147.
[16] R. Bodet, J. Lamon, N. Jia, R.E. Tressler, J. Am. Ceram. Soc. 79 (1996) 273.
[17] J.A. DiCarlo, H.M. Yun, G.N. Morscher, J.C. Goldsby, Ceram. Trans. 58 (1995) 43.
[18] G. Simon, A.R. Bunsell, J. Mater. Sci. 19 (1984) 3658.
[19] D.B. Marshall, B.N. Cox, A.G. Evans, Acta Metall. Mater. 38 (1985) 2013.
[20] C.H. Hsueh, J. Mater. Sci. 30 (1995) 1781.
[21] R.A. Lowden, Adv. Comp. Mater. (1991) 619.
[22] C.A. Lewinsohn, C.H. Henager Jr., R.H. Jones, submitted to J. Am. Ceram. Soc.
[23] N. Chawla, J.W. Holmes, J.F. Mansfield, Mater. Charact. 35 (1995) 199.
[24] C.H. Carter Jr., R.F. Davis, J. Bentley, J. Am. Ceram. Soc. 67 (1984) 732.